*Mon. Not. R. astr. Soc.* (1986) **223,** 377–389

# The peculiar shape of the inner galactic rotation curve

Ortwin E. Gerhard *Max-Planck-Institut für Physik und Astrophysik, Institut für Astrophysik, Karl-Schwarzschild-Straße 1, 8046 Garching b. München, Federal Republic of Germany*

Mario Vietri *Osservatorio Astrofisico di Arcetri, Largo E. Fermi 5, 50125 Firenze, Italy*

Accepted 1986 June 19. Received 1986 June 19; in original form 1986 April 1

**Summary.** The apparent galactic rotation curve as inferred from H I and CO terminal velocities shows a narrow peak ($v_{max} \simeq 250$–$260\,km\,s^{-1}$) at $r \simeq 500$ pc, and a steep decline for $600\,pc \leqslant r \leqslant 1.5$ kpc down to a rather broad minimum ($v_{min} \simeq 195\,km\,s^{-1}$) around 2.8 kpc. In this paper, we show that this morphology can be reconciled with the bulge density distribution determined by infrared observations *and* the local density of spheroid stars only if the bulge of our Galaxy is non-axisymmetric and the resulting potential triaxial.

In order to reproduce the galactic rotation curve satisfactorily, we require that the Sun be within 20° of the short axis of the bulge in the equatorial plane (the long axis of the closed loop orbits), and that the mean axial ratio of the bulge in the disc plane be 0.6 inside the knee in the density distribution at 800 pc. From such a viewing direction this simultaneously moves the peak in the apparent rotation curve inwards to 500 pc, and explains the near-Keplerian fall-off in terms of the rapidly decreasing quadrupole moment of the potential. For the same peak rotation velocity, our best-fitting bulge model has only 2/3 of the mass of a corresponding axisymmetric bulge.

In several external galaxies, the inner rotation curves show anomalies in the sense expected if the bulges of these systems were triaxial. In NGC 2708 and NGC 3054 we appear to observe the bulge from a direction near the plane containing the major and minor axes, and in NGC 3200 and UGC 2885 from near the plane containing the intermediate and minor axes. The apparent mass-to-light ratios of the bulge components inferred from the inner rotation curves will depend considerably on the viewing geometry in cases where the bulge is triaxial.

## 1 Introduction

The inner part ($r \leqslant 3$ kpc) of the galactic rotation curve is crucial to our understanding of the mass distribution, total mass, and shape of the galactic bulge. However, its peculiar morphology and

the detection of non-circular motions in this region (Oort 1977) have made this task especially difficult. The inner galactic rotation curve as derived from terminal velocities shows a narrow peak ($v_{max} \simeq 250$–$260\,km\,s^{-1}$, Burton & Gordon 1978; Knapp 1983) at $r \simeq 500\,pc$, and a steep decline for $600\,pc \leqslant r \leqslant 1.5\,kpc$ to a rather broad minimum ($v_{min} \simeq 195\,km\,s^{-1}$) around $r \simeq 2.8\,kpc$. This morphology is not unique to our Galaxy; a number of galaxies in the sample of Rubin, Ford & Thonnard (1980) and Rubin *et al.* (1982, 1985) show a similar pattern (e.g. NGC 4845 Sa, NGC 3200 Sb, UGC 2885 Sc).

The peak in the galactic rotation curve occurs in the 'nuclear disc' (Oort 1977), a region where the gas motion seems to be explainable in terms of pure rotation. The minimum has been seen both in H I (Burton & Gordon 1978) and in CO surveys (Burton & Gordon 1978; Clemens 1985). The peak is generally attributed to the gravitational influence of the bulge (Sanders & Lowinger 1972), but the steep, near-Keplerian decrease observed for $0.5\,kpc \leqslant r \leqslant 1.5\,kpc$, apparently implying an abrupt cut-off of the bulge (Bahcall, Schmidt & Soneira 1982), is difficult to reconcile with the smooth turnover of the bulge density distribution inferred from the 2.4-$\mu$m observations (Matsumoto *et al.* 1982). Furthermore, the existence of large non-circular motions of the gas in the bulge region has led Knapp (1983) and Burton (1983) to question the reality of the peak and then also of the following decrease.

However, hydrodynamical simulations by Mulder & Liem (1986) have shown that the gas-flow pattern in the plane of a rotating triaxial potential can, at least qualitatively, reproduce many features due to non-circular motions in the galactic $(l, v)$-diagram. That the bulge of our Galaxy might be triaxial has long been suggested (Kerr 1967); M31 probably has a prolate or triaxial bulge (Stark 1977; Gerhard 1986), and from studying isophote twists in nearby spiral galaxies it appears that this may not be uncommon (Zaritsky & Lo 1986). A non-axisymmetric bulge (we take this to include a prolate bulge with major axis in the plane of the disc) may have interesting effects on the apparent rotation curve of our Galaxy (Mulder 1986; Vietri 1986). A more detailed study of this effect is the purpose of this paper.

The gas flow in a non-axisymmetric potential may be approximately understood in terms of the gas moving on the available closed, stable, non-intersecting orbits in the equatorial plane (Sanders & Huntley 1976). Since these closed orbits are elongated, an observer looking along an orbit's major (minor) axis will see a higher (lower) velocity than the circular velocity at the same radius in an axisymmetric potential of the same mass. The apparent rotation curve is then determined by the run with radius of the mean velocity *and* the ellipticity of the gas streamlines (closed orbits) in the given potential. We consider here a galactic model consisting of an axisymmetric disc and a non-axisymmetric bulge whose density distribution and turnover radius are taken directly from infrared observations. We show that the apparent rotation curve in this potential fits well the observed shape of the galactic rotation curve, for an axial ratio of the bulge in the disc plane of 10:6, and a viewing direction within 20° of the intermediate axis. The principal features that give the observed rotation curve in this model are, (i) the turnover in the density profile outside which the closed orbits become rapidly round, and (ii) the existence of elongated loop orbits far inside this turnover, which is characteristic also of a de Vaucouleurs-type potential (Gerhard & Binney 1985), but not of a potential with harmonic core.

The plan of this paper is as follows: in Section 2 we describe our model of the galactic disc and bulge, and discuss the relevant observations and our assumptions. In Section 3, we show how a non-axisymmetric bulge with density profile fixed by infrared observations but with varying axial ratios modifies the galactic rotation curve, first by a linear analysis and then by numerical integrations of the relevant orbits in the various galactic models. We then fit these models to the observations and show that only a triaxial or prolate bulge is consistent with the galactic rotation curve. In Section 4 we discuss observational and theoretical uncertainties, the relation to previous work, and the application to external galaxies. Section 5 contains our conclusions.

## 2 Observations and model of the bulge and disc

The integrated light from the stars in the galactic bulge can be observed directly in the $K$-band ($2.2\mu$m); the apparent density distribution within $\lesssim 100$ pc is $\varrho \propto a^{-1.8}$ (Becklin & Neugebauer 1968). Here we have assumed an ellipsoidal model:

$$a^2 = x^2 + \frac{y^2}{\zeta^2} + \frac{z^2}{\xi^2}, \tag{1}$$

and $\zeta, \xi$ are the true axial ratios. Only $\xi$ is determined from the surface photometry; inside 50 pc*, $\xi \simeq 0.4$. Recent observations (Matsumoto *et al.* 1982) extending to $\sim 10°$ (1.5 kpc) from the Galactic Centre appear to join smoothly with the earlier data, confirming the $a^{-1.8}$ profile out to $a \simeq 800$ pc (from Matsumoto *et al.*'s fig 3 and fitting their 2.4-$\mu$m volume emissivity model). In this region, the observed axial ratio is now $\xi \simeq 0.75$. Beyond the turnover radius the bulge density distribution steepens considerably. The asymptotic slope beyond $a_{\rm knee}$ is not well determined by the data, which cover only an extra factor of 2 in radius, even though it is clearly $\varrho \propto a^{-3}$ or steeper. However, if we regard the spheroid stars in the solar neighbourhood as part of the galactic bulge, we can use the local density of the spheroid to constrain the bulge profile for $a > a_{\rm knee}$. Using an oblate $a^{-1.8}$ mass distribution for the inner bulge with axial ratio 0.7, and requiring that the maximum rotation velocity of the bulge alone be 247 km s$^{-1}$ (the value it has in the Bahcall *et al.* 1982 model), we find for the density at the knee of the bulge profile $\varrho_{\rm knee} = \varrho_b(a_{\rm knee} = 800\,{\rm pc}) \simeq 2.6\, M_\odot/{\rm pc}^3$. The limits on the local density of spheroid stars, $\varrho_b(r_\odot) = (0.4\text{–}1.7) \times 10^{-3}\, M_\odot/{\rm pc}^3$ (Schmidt 1983) then require a density profile between $a^{-3.1}$ and $a^{-3.7}$ beyond $a_{\rm knee}$, for a solar radius of 8.5 kpc. We therefore adopt for the bulge density distribution

$$\varrho_b = \begin{cases} \varrho_{\rm knee} \left( \dfrac{a}{a_{\rm knee}} \right)^{-1.8} & a < a_{\rm knee} = 800\,{\rm pc}, \\ \varrho_{\rm knee} \left( \dfrac{a}{a_{\rm knee}} \right)^{-3.5} & a > a_{\rm knee}, \end{cases} \tag{2}$$

with $\varrho_{\rm knee}$ fixed from the observed peak rotation velocity. The discontinuity in slope does not affect our results, because the force corresponding to (2) is smooth and the difference in mass from a model with more gentle turnover is small (see also Section 4). The axial ratios in the inner bulge are taken as free constants, but with the constraints $0.4 < \xi < 0.75$ from the $K$-band photometry, and $\zeta < \xi$ from the requirement that stable closed loop orbits exist in the disc plane, i.e. the shortest bulge axis coincides with the disc rotation axis.

For the galactic disc we take a model with an exponential surface density, $\sigma_{\rm D} = \sigma_0 \exp(-\alpha r)$, which is determined by the scale-length $\alpha^{-1} = 3.5$ kpc and the local disc surface density, $\sigma_{\rm D\odot} = 64\, M_\odot\,{\rm pc}^{-2}$ (Bahcall *et al.* 1982; Schmidt 1983). In the whole region of interest to us, the contribution of the dark halo to the potential is negligible and will be omitted. The last parameter to be fixed is the bulge figure rotation $\Omega_p$. We will argue in the following that any realistic value of $\Omega_p$ will not affect our results. Thus we simply set $\Omega_p = 0$ and postpone the discussion of this important parameter to Section 4.

*Throughout this paper, we assume a solar radius of 8.5 kpc.

## 3 The galactic rotation curve

### 3.1 ROTATION CURVES DUE TO BULGE MODELS OF VARIOUS SHAPES

In this section we discuss how the galactic rotation curve is modified by the introduction of a non-axisymmetric bulge. We treat the gas as a collisionless fluid orbiting the centre of the Galaxy on stable, closed, non-self-intersecting orbits in the principal plane of the bulge; this is a good approximation in the absence of shocks such as is expected in a non-rotating model, and will be discussed further in Section 4. In a non-rotating triaxial potential the only suitable orbits are the short-axis loops, which are elongated along the bulge intermediate axis (Binney 1982) by the potential's quadrupole moment. When viewed down its major axis (i.e. the potential's intermediate axis), the tangent point velocity of such an orbit will seem higher than that of a circular orbit at the same radius in a corresponding axisymmetric potential (Lake & Norman 1982) and the corresponding tangent point distance from the centre will equal its semi-minor axis length. Similarly, a lower velocity will be seen when the orbit is viewed down its short axis (the potential's long axis), and the tangent point distance will be equal to the orbit's semi-major axis length.

This can be made more quantitative by considering the first-order perturbation to circular orbits in the plane containing the long and intermediate axes of a weakly triaxial potential. In this plane we approximate the potential as

$$V\left(r, \theta=\frac{\pi}{2}, \phi\right)=V_0(r)+V_2(r)\cos 2\phi, \tag{3}$$

where $V_2$ is treated as a small perturbation. Then in first-order epicyclic approximation, i.e. writing $r=r_0+\delta r$, $\phi=\phi_0+\delta\phi$, $\phi_0=\Omega_0 t$ with $r_0\Omega_0^2=(dV_0/dr)_{r_0}$, the solution for the radial perturbation $\delta r$ from a circular orbit, which is periodic in $\phi_0$, can easily be shown to be

$$\delta r=-\frac{[2V_2(r_0)/r_0]+(dV_2/dr)_{r_0}}{\varkappa_0^2-4\Omega_0^2}\cos(2\phi_0), \tag{4}$$

where $\varkappa_0^2=3\Omega_0^2+(d^2V_0/dr^2)_{r_0}$ denotes the usual epicyclic frequency. The perturbation of the tangential velocity is obtained from

$$r_0\delta\dot{\phi}+2\Omega_0\,\delta r=-\frac{V_2(r_0)}{r_0\Omega_0}\cos(2\Omega_0 t). \tag{5}$$

If the long axis of the potential is taken to be at $\phi_0=0$, one must have $V_2(r)<0$ (equation 3); then for realistic potentials the numerator of (4) is positive. Since also $\Omega_0<\varkappa_0<2\Omega_0$, equation (4) shows that the perturbed closed orbits are elongated along the minor axis of the potential. The ellipticity is

$$\varepsilon_r\equiv 1-\frac{r_{\min}}{r_{\max}}\simeq\frac{2\,\delta r_{\max}}{r_0}=\frac{-2}{r_0\Delta^2}\left[\left(\frac{dV_2}{dr}\right)_0+\frac{2V_2(r_0)}{r_0}\right] \tag{6}$$

and the velocity contrast can be shown to be

$$\begin{aligned}\varepsilon_v\equiv 1-\frac{v_{\min}}{v_{\max}}&\simeq 2\left[\frac{\delta r_{\max}}{r_0}-\frac{V_2(r_0)}{r_0^2\Omega_0^2}\right]\\&=\frac{2}{r_0\Delta^2}\left[\frac{\varkappa_0^2-6\Omega_0^2}{\Omega_0^2}\,\frac{V_2(r_0)}{r_0}-\left(\frac{dV_2}{dr}\right)_0\right]\end{aligned} \tag{7}$$

from equation (5). Here, $\Delta^2 \equiv 4\Omega_0^2 - \varkappa_0^2$. Thus the orbital ellipticity and velocity contrast are directly determined by the potential's quadrupole moment.

Consider first as a simple example the (generalized) scale-free potential of Monet, Richstone & Schechter (1981)

$$V(r,\theta,\phi) = \frac{v^2}{2} \ln\left\{\frac{r^2}{r_0^2}\left[1 + \alpha P_2(\cos\theta) + \tfrac{1}{3}\eta P_2^2(\cos\theta)\cos 2\phi\right]\right\}. \tag{8}$$

In this case, for $\alpha$, $\eta \ll 1$ we have

$$\varepsilon_r \simeq \eta \tag{9a}$$

$$\varepsilon_v \simeq 2\eta, \tag{9b}$$

independent of (mean) radius $r_0$. For a mass model like the one adopted above for our Galaxy, a few significant differences occur. (i) Inside the knee in the bulge profile, the potential is effectively scale-free and we expect a constant orbital ellipticity. Outside $a_{\rm knee}$, however, the density profile falls off steeply, and while the monopole component of the potential approaches the Keplerian $1/r$-fall-off, the higher multipole moments die out faster. Hence the orbits become rapidly circular beyond $a_{\rm knee}$, with the effect that the apparent velocity difference between $\frac{1}{2}a_{\rm knee}$ and $2a_{\rm knee}$ is higher (lower) than in the corresponding axisymmetric case, depending on whether one looks down the orbit's major (minor) axis. (ii) In the axisymmetric bulge model the peak rotation velocity occurs at $a \simeq a_{\rm knee}$. However, a loop orbit in the non-axisymmetric counterpart begins to perceive the relative decrease of the quadrupole moment already when its semi-major axis exceeds $\sim q_\phi a_{\rm knee}$, where $q_\phi$ is the flattening of the potential contours. When looked at down its major axis, it will subsequently decrease its tangent velocity both because of the decrease in $M/r$ and because it becomes more circular. Hence we expect the maximum of the apparent rotation curve from this observing position to occur now at approximately $r \simeq (1-\varepsilon_r) q_\phi a_{\rm knee}$, i.e. significantly inward of $a_{\rm knee}$ as observed in the Galaxy.

In Fig. 1 we show the apparent rotation curves from loop orbits in four bulge models, all with the density profile of equation (2) but with differing axial ratios, as seen by an observer on the intermediate axis of the potential. The density distributions are normalized so as to give the same peak velocity. Notice that the asymptotic ($r \to \infty$) rotation curves for the non-axisymmetric

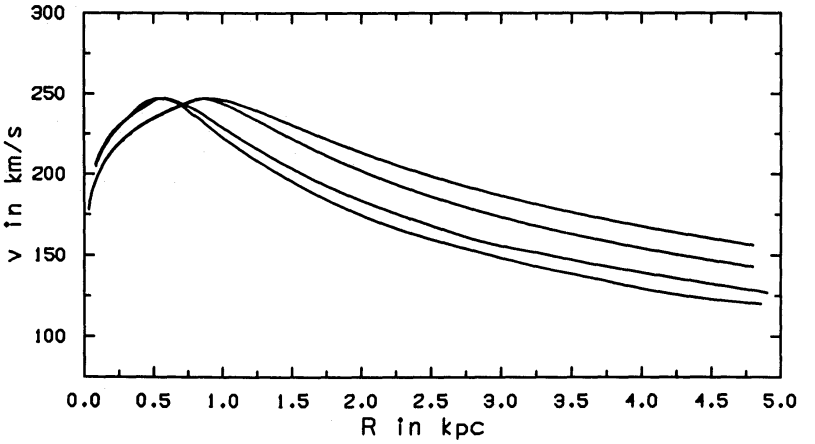


**Figure 1.** Rotation curves for four bulge models as seen from infinity along the potential's intermediate axis. All bulge models have the density distribution of equation (2), and are normalized to the same peak rotation velocity. From top to bottom at large radii: spherical bulge, oblate bulge (1:1:0,4), prolate bulge (1:0.7:0.7) and triaxial bulge (1:0.7:0.4).

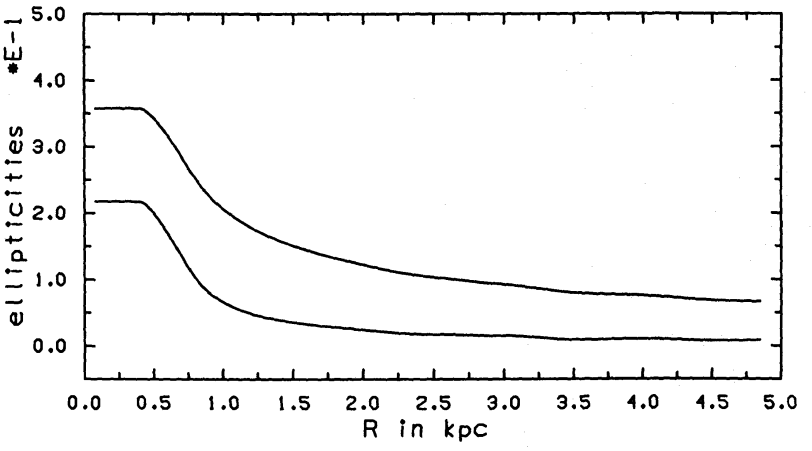


**Figure 2.** Orbital ellipticity $\varepsilon_r \equiv 1 - r_{\min}/r_{\max}$ (lower curve) and velocity contrast $\varepsilon_v \equiv 1 - v_{\min}/v_{\max}$ (upper curve), for closed short-axial loop orbits in the potential generated by the density distribution of equation (1) and axial ratios 1:0.6:0.6.

models are lower than for the axisymmetric models, because for this viewing direction less mass is required to achieve the same peak velocity. It is also apparent from Fig. 1 that in the non-axisymmetric cases the peak of the rotation curve has moved closer to the Galactic Centre, as discussed above. This allows one to reconcile the peak of the galactic rotation curve ($v_{\max} \simeq 250$–$260\,\mathrm{km\,s^{-1}}$, $r_{\max} = 500\,\mathrm{pc}$, Clemens 1985) with the observed position of the bulge cut-off ($a_{\mathrm{knee}} = 800\,\mathrm{pc}$, Matsumoto *et al.* 1982). This cannot be achieved even by a very flattened axisymmetric bulge with the observed density distribution, unless one introduces unphysical (and unobserved) cut-offs (Bahcall *et al.* 1982). Lastly, we notice that the fall-off outside the peak is slightly faster for the non-axisymmetric models, thus making the peak thinner and the decrease more nearly Keplerian.

The variation of the orbital ellipticity (which is responsible for these features) is displayed in Fig. 2, for loop orbits in the plane of the prolate galactic bulge model with axial ratios 10:6:6. Also shown is the resulting velocity contrast, which is typically two to three times larger than the orbital

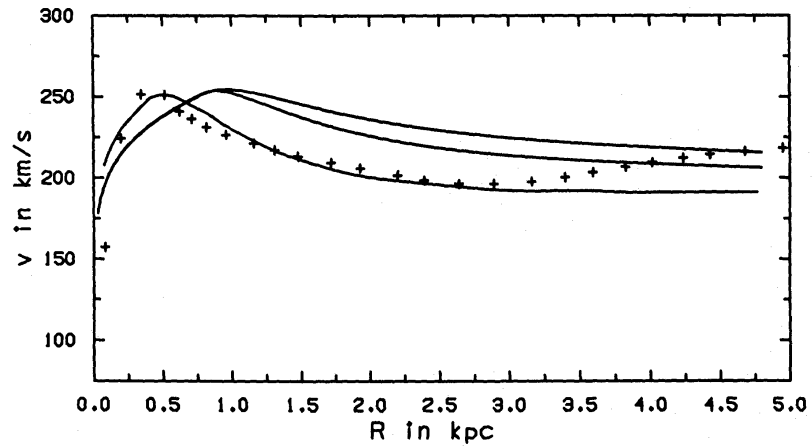


**Figure 3.** Apparent rotation curves (tangent velocities from infinity) along the intermediate axis, computed for three galactic bulge models plus standard galactic disc, and compared with observations. The plus signs are taken from a smooth curve drawn through the observations (from Clemens 1985). Curves from top to bottom at large radii: spherical bulge, oblate bulge (1:1:0.4), and prolate bulge (1:0.6:0.6).

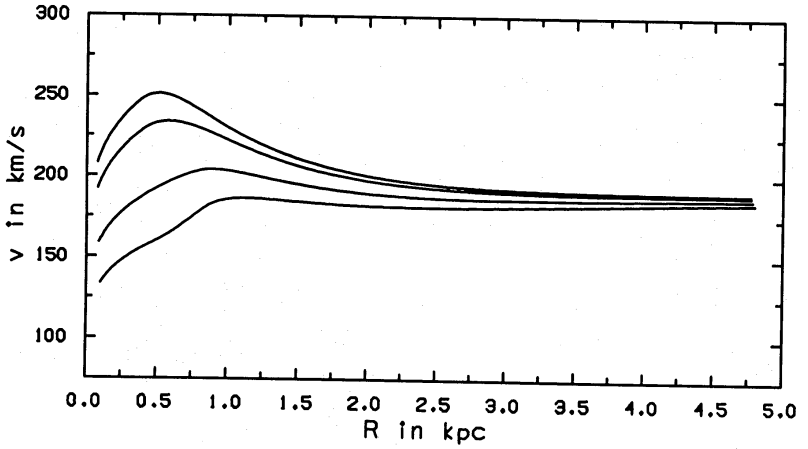


**Figure 4.** Tangent rotation curves in a prolate bulge (1:0.6:0.6) plus disc model, as seen by observers at different position angles relative to the bulge's intermediate axis. Curves are (from top) for $\phi=0°$, 20°, 45°, 90°.

ellipticity. The run of $\varepsilon_v/\varepsilon_r$ with radius can be understood simply. Suppose $V_0 \propto r^{p+2}$ and $V_2 \propto r^{q+2}$. Then from equations (6) and (7)

$$\frac{\varepsilon_v}{\varepsilon_r}=\frac{4-(p-q)}{4+q}. \tag{10}$$

For $r \ll a_{\text{knee}}$, the potential is self-similar, $p=q=-1.8$; then $\varepsilon_v/\varepsilon_r=1.8$ which, considering the neglect of the higher-order moments, compares well with $\varepsilon_v/\varepsilon_r=1.65$ from the numerical integrations. For $r \gg a_{\text{knee}}$, most of the mass lies inside $a_{\text{knee}}$, so that $V_0 \propto r^{-1}$, but the quadrupole moment from this part decreases like $r^{-3}$, while that due to the mass exterior to $a_{\text{knee}}$ only decreases like $r^{q+2}$, where $q=-3.5$ is the slope of the density profile outside $a_{\text{knee}}$. Then, for $r \gg a_{\text{knee}}$, $p=-3$, $q=-3.5$ and $\varepsilon_v/\varepsilon_r=7$, in agreement with the numerical asymptotic value.

How critical is it that the observer should be on the intermediate axis of the potential to see the effects on the apparent rotation curve discussed above? In the following sub-section, we will show (Fig. 4) that a range of ±20° around this axis gives the correct pattern; the figure is drawn for the model including the galactic disc for better reference.

### 3.2 COMPARISON WITH THE OBSERVED GALACTIC ROTATION CURVE

We now attempt to fit the rotation curve of our galaxy as derived from H I and CO terminal velocities (Burton & Gordon 1978; Clemens 1985) by the models discussed in Section 3.1. For the moment, we assume that the Sun is perfectly aligned with the intermediate bulge axis in the non-axisymmetric case. In Fig. 3 the apparent rotation curves as seen by an observer at infinity* are shown for the spherical, oblate 10:10:4 and prolate 10:6:6 bulge models including the disc component and are compared to the observations. The plus signs are taken directly from a smooth curve drawn through the H I and CO data points (Clemens 1985, fig. 3, $r_\odot=8.5$ kpc, $v_\odot=220\,\text{km s}^{-1}$).

It is clear that the axisymmetric models fail in two respects: (i) The peak in their rotation curves is at $\sim a_{\text{knee}}=800$ pc rather than at the observed 500 pc, and (ii) the subsequent fall-off is much too

* The difference between the apparent rotation curves as seen from infinity or $r_\odot=8.5$ kpc is everywhere smaller than $5\,\text{km s}^{-1}$. This is because at 500 pc it is of order $2/\pi \times 500/8500\,(v_{\max}-v_{\min}) \simeq 4\,\text{km s}^{-1}$, and because outside 500 pc the orbits become rapidly circular.

slow to reach the minimum at 2.8 kpc. On the other hand, the non-axisymmetric model fits quite well in both respects. We have not tried to optimize the fit by e.g. introducing a varying axial ratio (recall that the observed axial ratio may vary between 50 pc and 500 pc). Our main point here is that *the observed galactic rotation curve is consistent with the bulge density profile determined from 2.4 μm observations and the local density of spheroid stars only if the bulge is non-axisymmetric.*

We next show that it is not critical that the Sun be aligned with the bulge intermediate axis exactly. In Fig. 4, we plot the apparent rotation curves for observers at infinity and misaligned with this axis by $\phi=0°$, 20°, 45°, 90°. A range of position angles $-20°\lesssim\phi\lesssim20°$ seems acceptable for the solar position when the mass-to-light ratio of the bulge is adjusted to the same maximum velocity. Fig. 4 also shows dramatically the effect of flattening the orbits by only 20 per cent. The pronounced peak is absent for $\phi\gtrsim45°$ and the slope of the inner rise depends strongly on $\phi$.

We have also computed the apparent rotation curve in one model (10:6:6) including rotation of the bulge. For corotation with $v_c=220\,\mathrm{km\,s^{-1}}$ at 10 kpc, and the bulge density adjusted to the same maximum rotation velocity when measured by an observer in an inertial frame, this produced no noticeable effect on the shape of the inner rotation curve ($r<1.5$ kpc). There is some difference at larger radii; as is well known (Binney 1982), the prograde loop orbits in a rotating triaxial potential vanish at the inner Lindblad resonance. This is at 2.6 kpc in the potential of the disc and spherical part of the bulge in this model. The difference between the rotating and non-rotating models and possible implications are discussed further below.

## 4 Discussion

In the last sections, we have constructed a mass model for the Galaxy. We will now discuss further the observational data and assumptions that went into this model, and some implications of our results.

In the inner few kpc, the peculiar tangential motion of the LSR does not change the observed tangent velocities appreciably. However, if the LSR had an outward radial velocity as large as $\sim40\,\mathrm{km\,s^{-1}}$ with respect to the Galactic Centre, as has been suggested by Clube (1983) and as might be expected if the local closed orbits were not circular, then the northern rotation curve (Burton & Gordon 1978; Clemens 1985) would be correspondingly shifted in amplitude (although its shape inside 3 kpc would remain unchanged). We have therefore computed the mean solar motion with respect to the OH/IR stars within 0°.5 of the Galactic Centre (Winnberg *et al.* 1985). The velocities of these 33 stars are accurately known from VLA observations, and have an intrinsic dispersion of $\sigma\simeq70\,\mathrm{km\,s^{-1}}$. The mean velocity is $u=-1.9\,\mathrm{km\,s^{-1}}$ with rms error $\sigma_u=\sigma/\sqrt{33}=12.5\,\mathrm{km\,s^{-1}}$. This result is consistent with the zero mean solar velocity found with respect to all the OH/IR stars within $l<5°$, and with the radial velocity distribution of planetary nebulae (Baud *et al.* 1981). Effects of solar peculiar motion on the inner galactic rotation curve will therefore be small, consistent with the small ($\sim10\,\mathrm{km\,s^{-1}}$) observed north–south asymmetry (Knapp 1983).

We have also assumed implicitly throughout this paper that the maximum velocity along a given line-of-sight of fixed longitude is the tangent velocity to the corresponding elongated orbit, even if the shape of the orbits in the region considered changes with radius. This is clearly true when one looks down the orbit's major axis, and it can be shown to be true along the orbit's minor axis provided the velocity contrast satisfies $d\ln\varepsilon_v/d\ln r\lesssim4$ (for a flat rotation curve). Only if this condition is violated do the orbits change shape so rapidly that the tangent velocity of an elongated orbit becomes smaller than the velocity of a slightly larger circular orbit projected on to the same line-of-sight. In our galactic model the maximum value of the logarithmic derivative is $d\ln\varepsilon_v/d\ln r=0.8$, and in addition the mean rotation velocity decreases where the ellipticity of the orbits decreases; thus tangent point velocities are highest along any line-of-sight.

We have concentrated above on galactic mass models with no figure rotation. In gas-dynamical simulations of the galactic disc the pattern speed is usually chosen such that corotation lies at or somewhat outside the solar radius (e.g. Mulder & Liem 1986). It is clear that rotation of this magnitude does not significantly matter at ~500 pc so that our results concerning the maximum velocity and shape of the peak in the galactic rotation curve will be nearly independent of the assumed rotation rate. However, pattern rotation *does* change the shape of the closed orbits at and beyond the inner Lindblad resonance, which for corotation at 10 kpc and our galactic mass model is approximately at 2.5–3 kpc. Hydrodynamical simulations of gas-flow patterns in rotating triaxial potentials (Sanders & Huntley 1976; Mulder & Liem 1986) show that the shape of the streamlines changes at the ILR: inside the ILR, the streamlines are prograde loop orbits, which are elongated along the potential's intermediate axis, while outside the ILR they are long-axial loops, elongated along the potential's major axis (see Binney 1982 for the nomenclature of orbits). In a rotating triaxial potential, an observer on the potential's intermediate axis would therefore see a decrease in apparent rotation velocity which is larger than that in a non-rotating model of the same ellipticity, where the transition is only from prograde loop orbits to circular orbits.

Thus, in a rotating model, one might achieve the same difference in velocity between the peak and the minimum of the rotation curve with a slightly smaller bulge ellipticity ($\zeta$). Another difference to the non-rotating models is (Mulder & Liem 1986) that the spiral structure associated with the shocks in the gas flow at the ILR and other resonances gives rise to many features of non-circular motions in an $(l, v)$-diagram which may be made to resemble the observations. However, inspection of Mulder & Liem's results shows that this requires that the Sun be near the *major* axis of the potential, along which the apparent rotation velocities are *lower* than in the corresponding axisymmetric case. Thus the large rotation velocities observed in the nuclear disc and the features in the $(l, v)$-diagram cannot be simultaneously fitted by their model.

Furthermore, it is unclear whether the required figure rotation rates are consistent with observations. To sharpen the question, we have computed $\Omega(r)$ and $(\Omega-\varkappa/2)(r)$ in two galactic models including the disc component (the bulge had $\zeta=\xi=0.6$ or 0.8 and was normalized to $v_{\max}=247\,\mathrm{km\,s^{-1}}$). We find that in order to have the ILR at 2 kpc [where it is in the model of Mulder & Liem which best fits the $(l, v)$-diagram] we must have rotation rates that put corotation at between 7.3 and 8.0 kpc, i.e. inside the solar radius. Although direct measurements of the rotation of the galactic spheroid are not available to our knowledge, we can obtain an estimate of the pattern speed in a few external bulges with detailed kinematic data. Since the amount of counterstreaming allowed in a tumbling ellipsoidal stellar system is very limited (Vietri 1986), the linear part of the rotation curve gives an approximate upper limit to the figure rotation speed. Moreover, the contribution of figure rotation to the observed mean streaming velocity must be independent of $z$ and line-of-sight position in edge-on systems; in these galaxies we may therefore use slit measurements parallel to the major axis at large $z$ where contamination from a thick disc component is unimportant and the observed rotation is smallest.

Sufficient kinematic data exist for NGC 4565 Sb and NGC 7814 Sab (Kormendy & Illingworth 1982). From the largest $z$ parallel slit positions we estimate $r_{\mathrm{corot}}>320$ arcsec$\widehat{=}$15.6 kpc for NGC 4565 and $r_{\mathrm{corot}}>185$ arcsec$\widehat{=}$13.4 kpc for NGC 7814. Here we have used the distances adopted by van der Kruit & Searle (1981, 1982) and disc rotation velocities $v_c=270\,\mathrm{km\,s^{-1}}$ for NGC 4565 from Sancisi (1976) and $v_c=245\,\mathrm{km\,s^{-1}}$ for NGC 7814 from Bottinelli, Gouguenheim & Paturel (1980). In NGC 4565, corotation in terms of the well-defined disc scale-length is bounded by $r_{\mathrm{corot}}>2.9\,\alpha^{-1}$.

If these lower limits have any relevance for our Galaxy (which has a similar disc rotation velocity), they indicate that corotation should lie distinctly outside 8 kpc. We have therefore concentrated on non-rotating models, but we have computed apparent rotation velocities in a

rotating (10:6:6) model with corotation at 10 kpc. Normalizing to the same maximum rotation velocity as seen by an inertial observer (this implied a slight reduction of the bulge mass), we found that the position and shape of the peak in the rotation curve out to 1.5 kpc remained almost unchanged.

In a non-rotating model, the gas streamlines are well approximated by closed, non-intersecting particle orbits, because pressure effects are negligible (Oort 1977) and no shocks occur because the orbits change smoothly with radius. In such a model, the 3 kpc arm and similar radial-motion features would have to be explained in one of the following two ways. (i) The stellar disc has formed spiral arms which cause shocks in the gas (Shu, Milione & Roberts 1973). This is not unreasonable because Sellwood (1985) found that in the Galaxy model by Bahcall *et al.* (1982) the disc was indeed mildly unstable to two-armed spiral modes; (ii) If the spiral arms (which in the presence of a non-axisymmetric bulge might be stronger) are insufficient to explain the required non-circular velocities of $\sim 50\,\mathrm{km\,s^{-1}}$ at 3 kpc, a barred disc component would be required. This possibility is attractive both because Kormendy (1982) states that triaxial bulges and bars often go together and appear to be at roughly right angles, and because a bar orientated roughly perpendicular to the bulge would perhaps allow one to combine the results of Mulder & Liem (1986) and those presented here. In such a model, the peak in the rotation curve would be due to the bulge (viewed along its intermediate axis from the Sun) and the 3 kpc-arm and related features in the $(l, v)$-diagram due to the bar (viewed along its major axis). However, much more work needs to be done in order to see whether this possibility is viable.

J. P. Ostriker has pointed out to us that discs with central holes can likewise cause rapid fall-offs in the rotation curve, by effectively introducing a negative $v^2$ at radii close to the edge of the hole (Caldwell & Ostriker 1981). We have therefore subtracted (in $v^2$) the rotation curve of an oblate $q=0.6$ bulge model from the observed rotation curve, in order to find the required characteristics of the disc. The bulge model had the density distribution of equation (2) and a normalization such as to fit the peak velocity at 500 pc. In order to reproduce the observed rotation curve outside 500 pc, we find that the disc must then be truncated towards the centre at 1 kpc, over a radial range as narrow as ~200 pc. Such a sharp truncation at 1 kpc does not seem to be observed in the inner galactic gas distribution (e.g. Oort 1977), and would require a rather low radial velocity dispersion of the disc stars ($\sim 50\,\mathrm{km\,s^{-1}}$ at 1 kpc).

From Fig. 3 the model fitting the observed inner galactic rotation curves best has a prolate 10:6:6 bulge with major axis approximately perpendicular to the direction of the Galactic Centre from the Sun. This model provides a considerably better match to the observations than, e.g. a prolate 10:7:7 or a triaxial 10:7:4 bulge model, but we do not think that we can discriminate between a prolate or near-prolate triaxial bulge. It is interesting in this connection that Schmidt (1983) has claimed that the distribution of RR Lyrae stars observed by Oort & Plaut (1975) is consistent with a prolate model.

The remaining small discrepancies between the 10:6:6 model and the data are probably not significant, given only the possibility of spiral perturbations in the disc or non-planar motions (Liszt & Burton 1980). Furthermore, the match to the observations might be improved by considering radially varying bulge ellipticities. A mean axial ratio of 10:6 in the disc plane within 1 kpc, although more flattened than in the case of M31 (10:8:8; Gerhard 1986), is consistent with the observations of Becklin & Neugebauer (1968; $c/a=0.4$ at $\leqslant 50$ kpc) and of Matsumoto *et al.* (1982; $c/a=0.75$ at ~1 kpc), but the real ellipticities of the bulge in this region may be varying unless the measurements close to the Galactic Centre are contaminated by disc stars. This last possibility and the large uncertainty in the extinction towards the Galactic Centre have also led us to investigate a bulge model with a less steep central density profile (de Vaucouleurs profile $\varrho \propto r^{-3/4}$, Young 1976; Gerhard & Binney 1985). This has the effect of flattening the loop orbits inside $a_{\mathrm{knee}}$ more strongly (they would disappear in a harmonic potential), but also of decreasing

the monopole moment outside $a_{\rm knee}$. However, again the position and shape of the velocity peak in a properly scaled model were not changed significantly.

Our model differs from previous models in several important respects. In a study mostly aimed at the properties of the galactic halo (a component that we have not considered in this paper except in assuming tacitly that it provides any missing rotation velocity outside 3 kpc), Bahcall *et al.* (1982) had to truncate their axisymmetric bulge model abruptly at 1 kpc in order to model the steep fall-off at 1.5 kpc in the rotation curve, and then had to introduce a separate fourth component to account for the local spheroid stars. This is in accord with Fig. 3 which shows that no axisymmetric bulge model that also contains the spheroid stars can be reconciled with the observed rotation curve. A more physical cut-off in the bulge profile $1/(r^2+a^2)$ was used by Schmidt (1983), but he had to adopt $a=300$ pc; using the infrared data, this implies a variation of $M/L$ by a factor of 10 over a factor of 3 in radius. Only when the bulge is made non-axisymmetric, can the infrared observations, a constant $M/L$, the local density of spheroid stars and the galactic rotation curve be combined in a consistent picture.

A non-axisymmetric model, when viewed from the right range of position angles in the equatorial plane ($\pm 20°$ about the intermediate axis), needs less mass to achieve the same maximum rotation velocity. Table 1 lists for the various models considered, (i) the total mass of the bulge, (ii) the mass within the turnover $a_{\rm knee}=800$ pc, and (iii) the bulge density at $a_{\rm knee}$ and at the solar position. The density at the solar radius is given both for $\varrho \propto a^{-3.5}$ outside $a_{\rm knee}$ as inferred from comparing the oblate 10:7 model with the range of observed values (Schmidt 1983), and for $\varrho \propto a^{-3}$ which would be the preferred slope for a second iteration of the prolate 10:6:6 model. The difference in total mass between the models is typically of order 50 per cent. The total luminosity of the bulge inside $a_{\rm knee}$ from Matsumoto *et al.* (1982) and assuming the same colour as for the central bulge of M31 (Sandage, Becklin & Neugebauer 1969) is $8.0\times10^9\,L_{\odot,K}$ or $1.0\times10^9\,L_{\odot,B}$. Thus the 10:6:6 model has a mass-to-light ratio $M/L_K=0.8\,M_\odot/L_{\odot,K}$ or $M/L_B=7\,M_\odot/L_{\odot,B}$.

Finally, we discuss the application of our results to external galaxies. The rotation curves that would be observed along lines-of-sight parallel to the projected major or minor axes of the elongated orbits in a non-axisymmetric bulge are identical to the curves for $\phi=90°$ and $\phi=0°$ in Fig. 4, while in order to obtain the rotation curves for the intermediate cases one would here have to integrate the velocity field along the line-of-sight (rather than just use the tangent velocities). There are two cases (NGC 2708, NGC 3054) in the sample of Rubin *et al.* (1980) and Rubin *et al.* (1982) where the rotation curves obtained from the CCD photometry are too steep to fit the data in the bulge region (Kent 1986). Indeed, the bulges in these galaxies appear to require negative $M/L$ ratios. If these bulges were non-axisymmetric, such an effect would be expected if the line-of-sight were in the plane containing the major and minor axes of the potential. Conversely,

**Table 1.** Bulge parameters. Columns (1) to (4) give the bulge mass, the mass within $a_{\rm knee}=800$ pc, the density at $a_{\rm knee}$, and the local density at the solar radius, for the various models considered. Column (5) gives the local density for an asymptotic density profile $\varrho \propto a^{-3}$ instead of the usual $\varrho \propto a^{-3.5}$.

| Models | $\frac{M_{\rm TOT}}{10^{10}\,M_\odot}$ | $\frac{M(a<a_{\rm knee})}{10^{10}\,M_\odot}$ | $\frac{\varrho_{\rm knee}}{M_\odot\,{\rm pc}^{-3}}$ | $\frac{\varrho_\odot}{10^{-4}\,M_\odot\,{\rm pc}^{-3}}$ | $\frac{\varrho_\odot^{(-3)}}{10^{-4}\,M_\odot\,{\rm pc}^{-3}}$ |
|---|---|---|---|---|---|
| Spherical | 3.65 | 1.07 | 2.0 | 5.1 | 17.0 |
| Oblate (0.7) | 3.32 | 0.98 | 2.6 | 6.7 | 22.0 |
| Oblate (0.4) | 2.96 | 0.87 | 4.1 | 10.4 | 34.0 |
| Prolate (0.7) | 2.46 | 0.72 | 2.7 | 2.0 | 7.7 |
| Prolate (0.6) | 2.22 | 0.65 | 3.4 | 1.4 | 6.1 |
| Triaxial (1:0.7:0.4) | 2.16 | 0.63 | 4.2 | 3.1 | 12.0 |

two other galaxies in the sample (NGC 3200, UGC 2885) show strong peaks and subsequent steep fall-offs in their rotation curves just like in our Galaxy, which cannot be properly modelled with an axisymmetric bulge consistent with the CCD data (Kent 1986). This sharp bulge–disc transition occurs naturally in non-axisymmetric bulges when the line-of-sight is in the plane containing the intermediate and short axes of the potential. Thus non-axisymmetric bulges as are sometimes required by photometric data (e.g. in M31) may also be needed to explain the inner rotation curves in these galaxies.

## 5 Conclusions

(i) The presence of a non-axisymmetric bulge with a realistic density profile may affect the apparent rotation curve of a gaseous disc in its equatorial plane in two alternative ways. (i) When viewed from near its intermediate axis, it creates a narrow peak in the rotation velocity inside the knee in the density profile, with an associated rapid decrease outside the knee. This is due to the change of quadrupole moment and orbital ellipticity with radius in this region. (ii) On the contrary, when viewed from near its major axis, the peak is totally erased and the rotation curve rises even more slowly than in the corresponding axisymmetric model. Both affects are probably seen in some external galaxies, and the first in our Galaxy. These results are shown in Figs 1, 2 and 4.

(ii) The inner galactic rotation curve as derived from HI and CO terminal velocities can be reproduced (Fig. 3) by the disc and a bulge that is consistent with the observed infrared density profile (Matsumoto *et al.* 1982) and that includes the local density of spheroid stars, but only if the bulge is made non-axisymmetric and the Sun is within 20° of its intermediate axis. Our best-fitting model has axial ratios 10:6:6, a total mass of $M_{\rm tot}=2.2\times10^{10}\,M_\odot$, $M(a<800\,{\rm pc})=0.65\times10^{10}\,M_\odot$, and a mass-to-light ratio $M/L_B=7\,M_\odot/L_{B\odot}$. This conclusion is independent of the figure rotation of the bulge for realistic pattern speeds.

(iii) The characteristic morphology of a peak and subsequent near-Keplerian fall-off in the rotation curve is also shown by NGC 3200 and UGC 2885 (Rubin *et al.* 1980, 1982; Kent 1986), while the two galaxies NGC 2708 and NGC 3054 appear to show the opposite effect. Indeed, the rotation curves in these two galaxies rise so slowly, that dynamical fits require negative mass-to-light ratios in an axisymmetric model. Triaxiality of the bulge is thus important in modelling the rotation curves of at least a fraction of spiral galaxies, and may significantly affect the derived mass-to-light ratios.

## Acknowledgments

We thank Drs J. Binney, J. P. Ostriker and R. Sanders for helpful conversations and each other's directors for their hospitality during the course of this work.

## References

Bahcall, J. N., Schmidt, M. & Soneira, R. M., 1982. *Astrophys. J.*, **258,** L23.
Baud, B., Habing, H. J., Matthews, M. E. & Winnberg, A., 1981. *Astr. Astrophys.*, **195,** 171.
Becklin, E. E. & Neugebauer, G., 1968. *Astrophys. J.*, **151,** 145.
Binney, J. J., 1982. In: *Morphology and Dynamics of Galaxies,* p. 1, eds Martinet, L. & Mayor, M, Geneva Observatory, Geneva.
Bottinelli, L., Gouguenheim, L. & Paturel, G., 1980. *Astr. Astrophys. Suppl.*, **40,** 355.
Burton, W. B., 1983. In: *The Milky Way Galaxy, IAU Symp. No, 106,* p. 75, eds van Woerden, H., Allen, R. J. & Burton, W. B., Reidel, Dordrecht, Holland.
Burton, W. B. & Gordon, M. A., 1978. *Astr. Astrophys.*, **63,** 7.

Caldwell, J. A. R. & Ostriker, J. P., 1981. *Astrophys. J.,* **251,** 61.
Clemens, D. P., 1985. *Astrophys. J.,* **295,** 422.
Clube, S. V. M., 1983. In: *The Milky Way Galaxy, IAU Symp. No. 106,* p. 145, eds van Woerden, H., Allen, R. J. & Burton, W. B., Reidel, Dordrecht, Holland.
Gerhard, O. E., 1986. *Mon. Not. R. astr. Soc.,* **219,** 373.
Gerhard, O. E. & Binney, J. J., 1985. *Mon. Not. R. astr. Soc.,* **216,** 467.
Kent, S. M., 1986. *Astrophys. J.,* submitted.
Kerr, F. J., 1967. In: *Radio Astronomy and the Galactic System, IAU Symp. No. 31,* p. 169, ed. van Woerden, H., Reidel, Dordrecht, Holland.
Knapp, G. R., 1983. In: *Kinematics, Dynamics and Structure of the Milky Way,* p. 233, ed. Shuter, W. L. H., Reidel, Dordrecht, Holland.
Kormendy, J., 1982. *Astrophys. J.,* **257,** 75.
Kormendy, J. & Illingworth, G., 1982. *Astrophys. J.,* **256,** 460.
Lake, G. & Norman, C., 1982. In: *The Galactic Center, AIP Conf. No. 83,* p. 189, eds Riegler, G. R. & Blandford, R. D., American Institute of Physics, New York.
Liszt, H. S. & Burton, W. B., 1980. *Astrophys. J.,* **236,** 779.
Matsumoto, T., Hayakawa, S., Koizumi, H., Murakami, H., Uyama, K., Yamagami, T. & Thomas, J. A., 1982. In: *The Galactic Center, AIP Conf. No. 83,* p. 48, eds Riegler, G. R. & Blandford, R. D., American Institute of Physics, New York.
Monet, D. G., Richstone, D. O. & Schechter, P. L., 1981. *Astrophys. J.,* **245,** 454.
Mulder, W. A., 1986. *Astr. Astrophys.,* **156,** 354.
Mulder, W. A. & Liem, B. T., 1986. *Astr. Astrophys.,* **157,** 148.
Oort, J. H., 1977. *Ann. Rev. Astr. Astrophys.,* **15,** 295.
Oort, J. H. & Plaut, L., 1975. *Astr. Astrophys.,* **41,** 71.
Rubin, V. C., Burstein, D., Ford, W. K. & Thonnard, N., 1985. *Astr. Astrophys.,* **289,** 81.
Rubin, V. C., Ford, W. K. & Thonnard, N., 1980. *Astrophys. J.,* **238,** 471.
Rubin, V. C., Ford, W. K., Thonnard, N. & Burstein, D., 1982. *Astrophys. J.,* **261,** 439.
Sancisi, R., 1976. *Astr. Astrophys.,* **53,** 159.
Sandage, A. R., Becklin, E. E. & Neugebauer, G., 1969. *Astrophys. J.,* **157,** 55.
Sanders, R. H. & Lowinger, T., 1972. *Astr. J.,* **77,** 292.
Sanders, R. H. & Huntley, J. M., 1976. *Astrophys. J.,* **209,** 53.
Schmidt, M., 1983. In: *The Milky Way Galaxy, IAU Symp. No. 106,* p.75, eds van Woerden, H., Allen, R. J. & Burton, W. B., Reidel, Dordrecht, Holland.
Sellwood, J. A., 1985. *Mon. Not. R. astr. Soc.,* **217,** 127.
Shu, F. M., Milione, V. & Roberts, W. W., 1973. *Astrophys. J.,* **183,** 819.
Stark, A. A., 1977. *Astrophys. J.,* **213,** 368.
van der Kruit, P. C. & Searle, L., 1981. *Astr. Astrophys.,* **95,** 105.
van der Kruit, P. C. & Searle, L., 1982. *Astr. Astrophys.,* **110,** 61.
Vietri, M., 1986. *Astrophys. J.,* in press.
Winnberg, A., Baud, B., Matthews, H. E., Habing, H. J. & Olnon, F. M., 1985. *Astrophys. J.,* **291,** L45.
Young, P. J., 1976. *Astr. J.,* **81,** 807.
Zaritsky, D. & Lo, K. Y., 1986. *Astrophys. J. Lett.,* submitted.